THÈSE PRÉSENTÉE

POUR OBTENIR LE GRADE DE

DOCTEUR

DE L'UNIVERSITÉ DE BORDEAUX

ECOLE DOCTORALE SCIENCES PHYSIQUES ET DE

L'INGÉNIEUR

LASERS, MATIÈRE, NANOSCIENCES

Par **Maxime Lavaud**

Confined Brownian Motion

Sous la direction de : **Thomas Salez**
Co-directrion : **Yacine Amarouchene**

Soutenue le 25 décembre 2019

Membres du jury :

Mme. Aude ALPHA	Directrice de Recherche	Université	Rapporteur
M. Bernard BETA	Directeur de Recherche	Université	Rapporteur
M. Georges GAMMA	Directeur de Recherche	Université	Président
Mme. Dominique DELTA	Chargée de Recherche	Université	Examinatrice
M. Eric EPSILON	Ingénieur de Recherche	Université	Examinateur
Mme. Jane DOE	Directrice de Recherche	Université	Directrice
Mme. Simone UNTEL	Ingénieure de Recherche	Université	Invitée

Abstract

Lorem ipsum dolor sit amet, consectetuer adipiscing elit. Ut purus elit, vestibulum ut, placerat ac, adipiscing vitae, felis. Curabitur dictum gravida mauris. Nam arcu libero, nonummy eget, consectetuer id, vulputate a, magna. Donec vehicula augue eu neque. Pellentesque habitant morbi tristique senectus et netus et malesuada fames ac turpis egestas. Mauris ut leo. Cras viverra metus rhoncus sem. Nulla et lectus vestibulum urna fringilla ultrices. Phasellus eu tellus sit amet tortor gravida placerat. Integer sapien est, iaculis in, pretium quis, viverra ac, nunc. Praesent eget sem vel leo ultrices bibendum. Aenean faucibus. Morbi dolor nulla, malesuada eu, pulvinar at, mollis ac, nulla. Curabitur auctor semper nulla. Donec varius orci eget risus. Duis nibh mi, congue eu, accumsan eleifend, sagittis quis, diam. Duis eget orci sit amet orci dignissim rutrum.

Table of Contents

List of Figures

Nomenclature

α Noise amplitude

ℓ_{B} Boltzmann length

ℓ_{B} Debye length

η Fluid viscosity

$\eta_\perp$ Viscosity orthogonal to a wall, see Eq.1.1.26

$\eta_\parallel$ Viscosity parrallel to a wall, see Eq.1.1.27

γ Friction coefficient

ρ_{F} Fluid density

ρ_{P} Particle density

B Amplitude of the electrostatic interactions

D Diffusion coefficient, see Eq.**??**

g Gravity constant

k_{B} Boltzmann Constant

m Mass of a particle

N_{A} Avogrado constant

R Gas constant

T Temperature

V_t Velocity of a particle

X_t Particle position, see Eq.**??**

List of Abbreviations

fps   Frames per second

MRSE   Mean Relative Squared Error

MSD   Mean Squared Displacement

PDF   Probability Density Function

RICM   Reflection Interference Contrast Microscopy

SDE   Stochastic Differential Equations

1   Stochastic inference of surface-induced effects using Brownian motion

1.1   Confined Brownian motion theory

By observing the trajectory along the z axis of a particle of 1.5 μm as shown on the fig.1, one can see that the particle height does not get heigher than $\simeq$ 4 μm. Indeed due to gravity, the particle is confined near the surface. Brownian motion in confinement and at interfaces is a canonical situation, encountered from fundamental biophysics to nanoscale engineering. This confinement induces near-wall effects, such as hindered mobility and electrostatic interactions.

In the first part of this chapter, I will detail the theory background of the confined Brownian motion and how to numerically simulate it. In a second part, I will present how to analyse experimental data. In particular, I will detail a multi-fitting procedure that allows a thermal-noise-limited inference of diffsion coefficients spatially resolved at the nanoscale, equilibrium potentials, and forces at the femtomewton resolution.
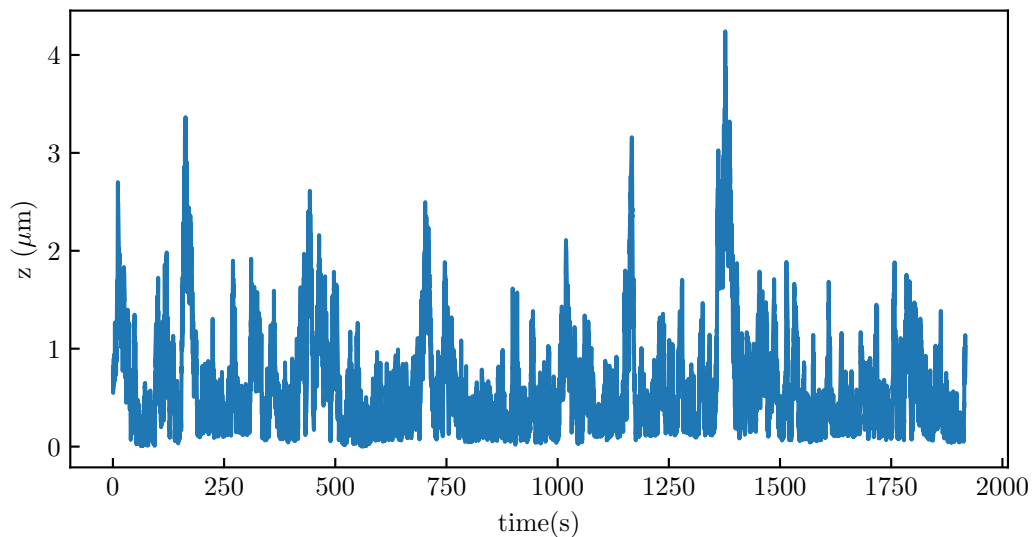

Figure 1: Experimental trajectory of a particule of polystyrene of radius $a = 1.5$ μm near a wall ($z = 0$) along the z axis — perpendicular to the wall.

1.1.1 Gravitational interactions

In our experiment, we observe confined Brownian motion since the colloids are subject to gravity. Indeed, the density of the observed colloid ρ_p is different of the medium ρ_m — in our experiment water, $\rho_\mathrm{m} = 1000$ kg.m^{-3}. Thus, the particle lies into a gravitational potential given by:

$$U_\mathrm{g}(z) = \Delta m g z = \frac{4}{3} \pi a^3 g \Delta \rho z \ , \tag{1.1.1}$$

where Δm is the mass difference of the particle and a fluid sphere of the same size, $\Delta \rho$ the corresponding density difference such as $\Delta \rho = \rho_\mathrm{m} - \rho_\mathrm{p}$ and g the gravitational acceleration. By invoking the definition of a distance that we call the Boltzmann length,

$$\ell_\mathrm{B} = \frac{k_\mathrm{B} T}{4/3 \pi a^3 \Delta \rho g} \ , \tag{1.1.2}$$

one can rewrite the gravitational potential Eq.1.1.1 as:

$$U_\mathrm{g} = \frac{k_\mathrm{B} T}{\ell_\mathrm{B}} \ . \tag{1.1.3}$$

The Boltzmann length ℓ_B is the typycal gravitational decay length and represents the balance between the gravital potential and thermal energy. This distance was first measured by Perrin [5], by enumerating the number of particles as a function of height to reconstruct the concentration of the colloidal suspension that exponentially decays as e^{-z/ℓ_B}. As an exemple, in water, for a particle polystyrene, $\rho_\mathrm{p} = 1050$ kg.m^{-3} and of radius $a = 1.5$ μm we have $\ell_\mathrm{B} = 0.58$ μm.

For particle with $\ell_\mathrm{B} >> a$, one can consider that the particle does not feel the gravity. This is particulary the case when the density of the colloids and fluid matches, in this particular case $\ell_\mathrm{B} = 0$. Thus density matching can we a way to do grativation free experiments. In the case of our experiment, we want to measure confinement induced effects, therefore, we need this gravitational interaction to have the particles near the surface. Indeed, as a particle gets larger, or, denser ℓ_B decreases and the particle will be, in average, closer to the surface.

1.1.2 Sphere-wall interactions

As we have seen, external forces acts on the particle such as the gravity, however it is not the only one. As the Brownian particle is close to a wall we can expect some interactions between the surfaces. In our case, we suppose that the Brownian particles do not interact between each other, which is the case for the dilute solution used. Indeed, the particles studied are at a minimum 50 μm apart which correspond to 10 times their size for the larger beads.

To describes the interaction between, the Brownian particle and the wall, we use the DLVO[1] theory. This theory was first developed to describe the interactions between colloids to explain the stability of colloidal suspension. It describes the interactions using two forces components; the Van Der Waals force which arise form the interactions between surface's molecules and electrostatic interactions due the a double-layer formed with the ions present in the solution.

Double-Layer interactions

When a surface is immersed in water are usually charged [68] due to a high dielectric constant $\epsilon \simeq 80$ that permit the build up of charges for low energetic price. Commonly, surface charging is done through ionization of dissociation of surface groups[2], from the binding of ions from the solution — for example, adsorption of $-OH^-$ onto the water-air interface that charge it negatively. In the bulk, a fluid should be electrically neutral, thus the fluid contains as many ions of opposite charge. However, when a surface is charged negatively, negative ions are repelled from the surface, while positive ions are attracted towards the surface. Therefore, a double-layer charge distribution is formed near the surface, as shown Fig.XX. Experimentally, we use glass slides and polystyrene beads, that are both negatively charged in water, thus leading to repulsive double-layer. This repulsive force prevent the colloids to stick together or to the surface of the substrate.

If the solution contains an electrolyte (ions of positive and negative charges), for example a salty solution, containing Na^+ and Cl^- ions. In the DLVO theory, the electrostatic field $\Psi(\vec{r})$ generated by the double layer satisfies the mean field Poisson's equation [68]:

---

[1] The DLVO theory is named after Derjaguin, Landau, Verwey, and Overbeek [68].

[2] For example, the dissociation of protons from surface carboxylic groups [68] ($-COOH \rightarrow -COO^- + H^+$) which charge negatively the surface.
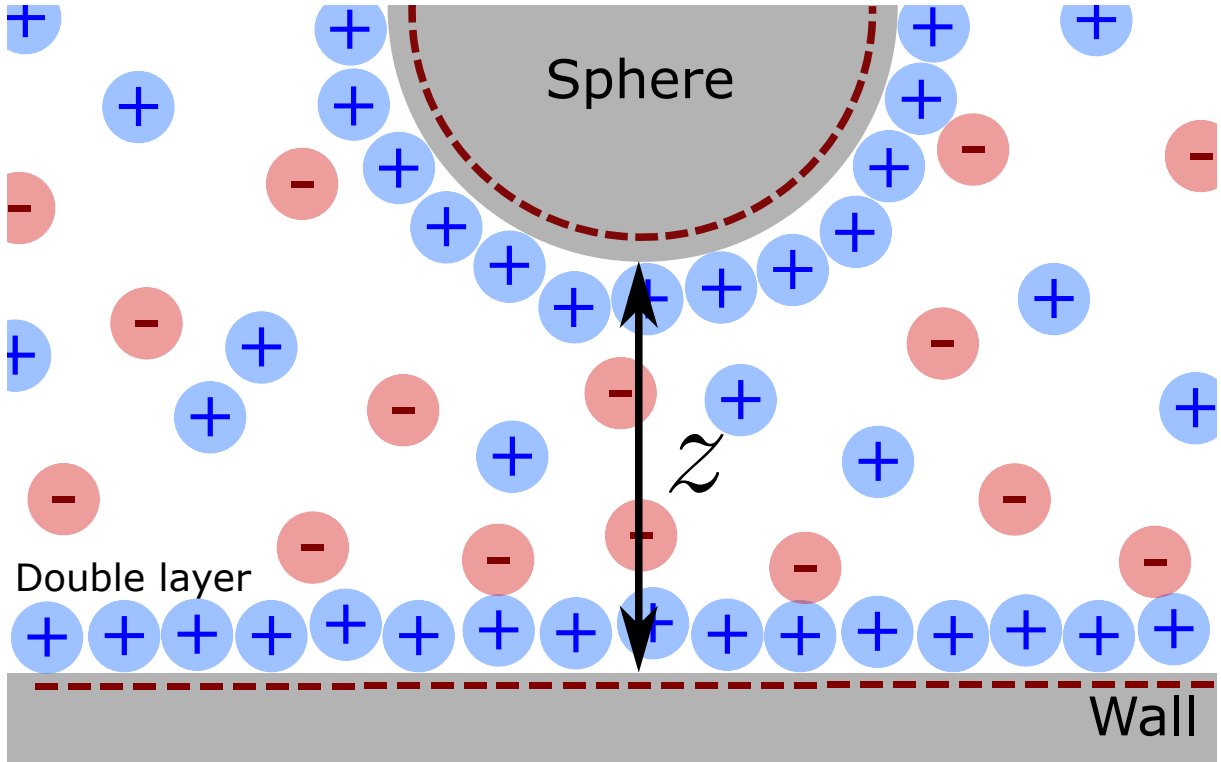
Figure 2: A Brownian colloid diffusing near a wall. Both wall and colloid's surface charge negatively, in consequence, a layer of positively charge ions are towards the surfaces, forming a double-layer charge distribution.

$$\nabla^2 \Psi(\vec{r}) = -\frac{1}{\epsilon_r \epsilon_0} \rho_e(\vec{r}) \ , \tag{1.1.4}$$

where ϵ_0 the vacuum permittivity, ϵ_r the relative permitivity of the fluid, $\rho_e(\vec{r})$ the local charge density. The latter can be written as:

$$\rho_e(\vec{r}) = e \sum_i z_i c_i(\vec{r}) \ , \tag{1.1.5}$$

where e is the elementary charge, i denotes an ionic species of valence z_i and local ionic concentration $c_i(\vec{r})$ (number density). If the solution is at the thermodynamic equilibrium, the Boltzmann equation is used to calculate the local ion density such that:

$$c_i(\vec{r}) = c_i^0 \exp\left(\frac{z_i e \Psi(\vec{r})}{k_{\mathrm{B}} T}\right) \ , \tag{1.1.6}$$

where c_i^0 is the bulk concentration (number density) of the ionic species i. By combining Eqs.1.1.4, 1.1.5 and 1.1.6, one can obtain the Poisson-Boltzmann equation:

$$\nabla^2\Psi(\vec{r}) = \sum_i \frac{z_i e c_i^0}{\epsilon_0\epsilon_r} \exp\left(-\frac{z_i e\Psi(\vec{r})}{k_{\mathrm{B}}T}\right) \ . \tag{1.1.7}$$

Since the Poisson-Boltzmann is non-linear, it is most likely to be solve numerically. However, for simple geometry such as uniformly charged plane or sphere it can be solve analiticaly. Let consider, to simplify, that we have a monovalent electrolyte, meaning that the electrolyte is composed of two ions of valence equal to one — Na^+ Cl^- for example — and c_i^0 is equal to the electrolyte solution concentration c_s^0. In that case Eq.1.1.7 simplifies to:

$$\begin{aligned}\nabla^2\Psi(\vec{r}) &= \frac{e c_s^0}{\epsilon_0\epsilon_r}\left[\exp\left(\frac{-e\Psi(\vec{r})}{k_{\mathrm{B}}T}\right) - \exp\left(\frac{+e\Psi(\vec{r})}{k_{\mathrm{B}}T}\right)\right] \\ &= 2\frac{e c_s^0}{\epsilon_0\epsilon_r}\sinh\left(\frac{e\Psi(\vec{r})}{k_{\mathrm{B}}T}\right) \ .\end{aligned} \tag{1.1.8}$$

In the case, where the Ψ is small enough everywhere to have the electrostatic potential energy $e\Psi << k_{\mathrm{B}}T$, which generally the case when using salty solution. In that case, it is possible, using the a Taylor approximation at the second order to write:

$$\exp\left(-\frac{z_i e\Psi(\vec{r})}{k_{\mathrm{B}}T}\right) \simeq 1 + \frac{z_i e\Psi(\vec{r})}{k_{\mathrm{B}}T} \ . \tag{1.1.9}$$

Thus, the Poisson-Boltzmann equation (Eq.1.1.7) becomes:

$$\nabla^2\Psi(\vec{r}) = \sum_i \frac{z_i e c_i^0}{\epsilon_0\epsilon_r}\left(1 + \frac{z_i e\Psi(\vec{r})}{k_{\mathrm{B}}T}\right) \ . \tag{1.1.10}$$

Since the fluid in the bulk, is electrically neutral, the first term vanishes as $\sum_i z_i c_i^0 = 0$. One thus have a linearized version of Eq.1.1.7, which is known as the Debye-Hünkel equation:

$$\nabla^2\Psi(\vec{r}) = \left[\sum_i \frac{z_i^2 e^2 c_i^0}{\epsilon_0\epsilon_r k_{\mathrm{B}}T}\right]\Psi(\vec{r}) \ . \tag{1.1.11}$$

From this approximation, one can identify that the term between brackets is the inverse of a distance squared. We can thus define a distance ℓ_{D}, the Debye length such as:

$$\ell_D = \sqrt{\sum_i \frac{\epsilon_0 \epsilon_r k_B T}{z_i^2 e^2 c_i^0}} \ . \tag{1.1.12}$$

The Debye length is the characteristic length of the double-layer, and, the electrostatic interactions. For a monovalent electrolyte, at 25 °C (298 K), the Debye length of aqueous solution is:

$$\ell_D = \sqrt{\frac{\epsilon_0 \epsilon_r k_B T}{2 c_s^0 e^2}} = \sqrt{\frac{8.854 \times 10^{-12} \times 78.4 \times 1.381 \times 10^{-23} \times 298}{2 \times (1.602 \times 10^{-19})^2 \times 6.022 \times 10^{26} M}} \tag{1.1.13}$$
$$= 0.304 \times 10^{-9} / \sqrt{M} \ \text{m} \ ,$$

with M the molar concentration (1 M = 1 mol.L^{-1} corresponding to a number density of $c_s^0 = 6.022 \times 10^{26}$ m^{-3}). Thus, for a salty concentration we have $\ell_D = 0.304/\sqrt{[\text{NaCl}]}$ nm. For exemple, for NaCl solution, one can have $\ell_D = 100$ nm for a concentration [NaCl] = 9.2 μM and $\ell_D = 10$ nm for a concentration [NaCl] = 9.2 mM.

Finally, the Debye-Hünkel approximation finally writes:

$$\nabla^2 \Psi(\vec{r}) = \kappa^2 \Psi(\vec{r}) \ , \tag{1.1.14}$$

with $\kappa = 1/\ell_D$. Using the latter approximation one can compute the electrostatic potential around a sphere. Let us consider a perfect sphere of radius a and charge Qe of charge density $\sigma = Qe/4\pi a^2$. With Q beeing the number of charge on the surface. Since the system has a spherical symmetry, one has $\Psi(\vec{r}) = \Psi(r)$ with $r = |\vec{r}|$. Using the Laplacian operator ∇^2 in the spherical coordinates, Eq.1.1.14 writes:

$$\frac{1}{r^2} \left[\frac{\partial}{\partial r} \left(r^2 \frac{\partial \Psi(r)}{\partial r} \right) \right] = \kappa^2 \Psi(r) \ , \tag{1.1.15}$$

which has a general solution:

$$\Psi(r) = C_1 \frac{\exp(\kappa r)}{r} + C_2 \frac{-\exp(\kappa r)}{r} \tag{1.1.16}$$

For one sphere, the electrostatic field vanishes at infinity such as $C_1 = 0$, such it has the form of a Yukawa potential:

$$\Psi(r) = C_2 \frac{-\exp(\kappa r)}{r} \ . \tag{1.1.17}$$

Additionally, at the surface of a charged sphere, the eletrostatic potential satifies:

$$\left. \frac{\partial \Psi(r)}{\partial r} \right|_{r=a} = \frac{Qe}{4\pi\epsilon_0\epsilon_r a^2} = \frac{\sigma}{\epsilon_0\epsilon_r} \ . \tag{1.1.18}$$

By applying the latter boundary condition to Eq.1.1.17 we find:

$$\Psi(r) = \frac{\sigma a^2}{\epsilon_0\epsilon_r} \frac{\exp(\kappa a)}{1 + \kappa a} \frac{\exp(-\kappa r)}{r} \tag{1.1.19}$$

This solution can be used to determine the electrostatic field between two spheres. Indeed, if we suppose that the presence of a second sphere, do not interfere with the distribution of ions in the double layer of the other. We can thus use the superposition approximation to write the potential $\Psi_2(z)$ between two spheres surfaces. Where z is the distance between the 2 colloids. For two spheres of charge σ_1 and σ_2 and radius a_1 and a_2, $\Psi_2(z)$ writes [69]:

$$\Psi(z) = \frac{4\pi}{\epsilon_0\epsilon_r} \left(\frac{\sigma_1 a_1^2}{1 + \kappa a_1} \right) \left(\frac{\sigma_2 a_2^2}{1 + \kappa a_2} \right) \frac{\exp(-\kappa z)}{a_1 + a_2 + z} \ . \tag{1.1.20}$$

From the latter equation, it is possible to write the electrostatic field between a wall and a spherical colloid, by setting one of the radius to infinity. Doing so and mulitplying by e, one can have the eltrostatic potential $E_{\mathrm{elec}}(z)$ between a Brownian particle and the wall:

$$E_{elec}(z) = B\mathrm{e}^{-\frac{z}{\ell_{\mathrm{D}}}} \ . \tag{1.1.21}$$

Where B is the constant that represent the surface charges, for sphere of radius a and charge σ_1 and a wall of charge σ_2, one has:

$$B = \frac{4\pi}{\epsilon_0\epsilon_r} \left(\frac{\sigma_1 a^2}{1 + \kappa a} \right) \frac{\sigma_2}{\kappa} \ . \tag{1.1.22}$$

Typical values for B ranges from 1 $k_{\mathrm{B}}T$ to 50 $k_{\mathrm{B}}T$. In our study we will keep B to describe

the electrostatic energy potential as it complicated to decouple the σ_1 and σ_2 when the colloid and wall's surface materials are different [70]. However, this is not impossible and is the idea of future work.
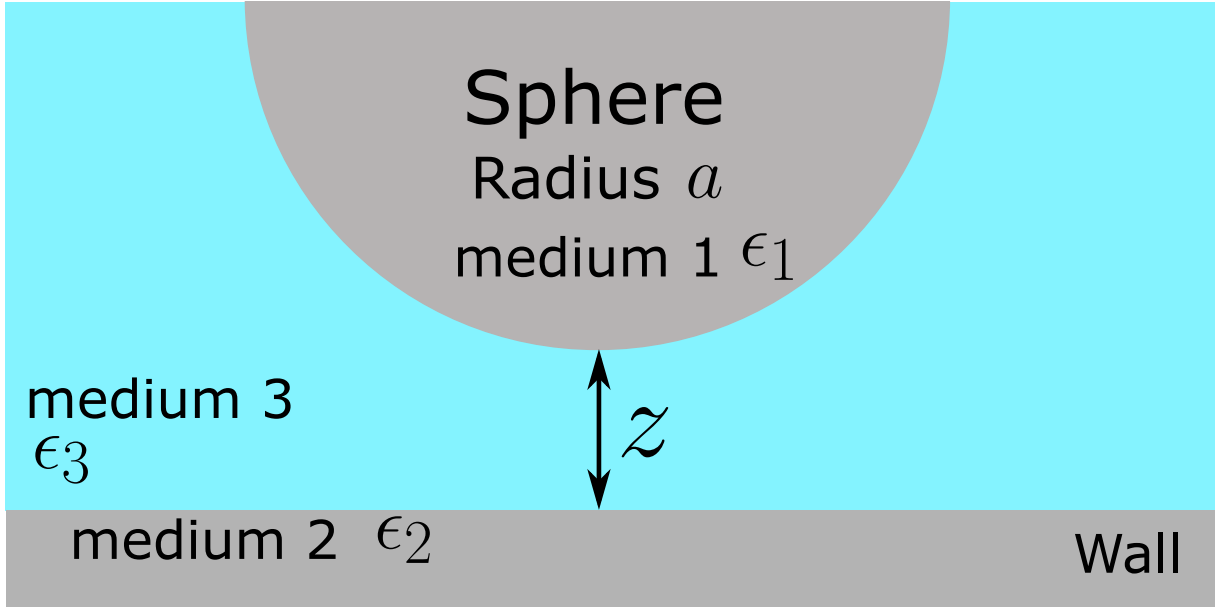
Van der Waals interactions

Figure 3: A colloid of radius a separated from a wall from a distance z. The colloid material has a static dielectric constant ϵ_1, the wall ϵ_2 and the solution ϵ_3.

In the DLVO theory, the Van der Waals forces describes the interaction between colloids at very short range. This forces are mainly attractive and in our case having Van der Waals interactions would lead to the particles stick to the wall. The Van der Waals potential energy E_{VdW} for a spherical colloid of radius a, at a height z at a few nanometers (< 5 nm) to the surface [68]:

$$E_{VdW} = -\frac{Aa}{6z} \qquad (1.1.23)$$

where A is the retarded Hamaker constant. For our system, where the particle, medium and wall are different medium as schematize in Fig.3. In that case the Hamaker constant writes [68]:

$$A = \frac{3}{4}k_{\mathrm{B}}T \left(\frac{\epsilon_1 - \epsilon_3}{\epsilon_1 + \epsilon_3}\right) \left(\frac{\epsilon_2 - \epsilon_3}{\epsilon_2 + \epsilon_3}\right) + \frac{3h}{4\pi} \int_{\nu_1}^{\infty} \left(\frac{\epsilon_1(i\nu) - \epsilon_3(i\nu)}{\epsilon_1(i\nu) + \epsilon_3(i\nu)}\right) \left(\frac{\epsilon_2(i\nu) - \epsilon_3(i\nu)}{\epsilon_2(i\nu) + \epsilon_3(i\nu)}\right) \mathrm{d}\nu \ ,$$

(1.1.24)

where ϵ_1, ϵ_2 and ϵ_3 are the static dieletric constants of the three media, $\epsilon(i\nu)$ are the imaginary dieletric constant at a frequency ν and $\nu_n = (2\pi k_{\mathrm{B}}Tn/h = 4 \times 10^{13}ns^{-1}$ at 300 K; and; h is the Plank's constant. The first term fives the zero-frequency energy of the van der Waals interaction and the second term the dispersion energy. However, since the static dielectric of water is large compared to the other medium, one can approximate the Hamaker constant of our system to only the zero-frequency term:

$$A = \frac{3}{4}1.381 \times 10^{-23} \times 298 \left(\frac{2.5 - 80}{2.5 + 80}\right) \left(\frac{5 - 80}{5 + 80}\right) \simeq 2.48 \times 10^{-21}\mathrm{J} = 0.62 \ k_{\mathrm{B}}T \quad (1.1.25)$$

Since A is positive we correctly have an attractive Van der Waals force, this case will always be the case due to the high dielectric constant of water. More over, the zero-frequency Van der Waals force is mainly due to electrostatic interaction and is thus screened by electrolytes, we thus need to add a factor $\approx e^{-z/\ell_D}$ to the Van der Waals forces. Finally, to have the force at higher distances one should add a second factor to account for the retarded Van der Waals force of $\simeq (1 + 11z/100\mathrm{nm})^{-1}$ [68]. All the effects added together we can see that the Van der Waals forces will play a role only a few nanometer (< 10 nm). In our experiments, the Debye length ℓ_{D} (> 20 nm) is large enough for the particle to avoid this region, in the following of this work the Van der Waals interactions will be neglected. To study the Van der Waals interactions with Brownian motion, it is possible, if one add enough salt to have $\ell_{\mathrm{D}} \simeq 1$ nm. With such a short Debye length, all the colloids would stick to the surface and together.

1.1.3   Local diffusion coefficient

We have seen that the bulk Brownian motion is well known and documented for a long time. But, in the real world, the boundaries are not at infinity and could play a role in the process of diffusion. Indeed, it was theorized by H. Faxen [71] that the presence of a wall would change the Stokes-Einstein relation with a viscosity dependent to the position of the particle. As the particle get closer to a surface, the presence of the non-slip boundary condition make the fluid harder to push, thus increasing the local viscosity of the particle.

This variation of the viscosity will be different for orthogonal and parallel displacement to the wall, thus we write respectively $\eta_\perp$ and $\eta_\parallel$ with η_0 being the fluid viscosity and z the height of the particle:

$$\eta_\perp = \frac{4}{3}\eta_0 \mathrm{sinh}\beta \sum_{n=1}^{\infty} \frac{n(n+1)}{2n-12n+3} \left[\frac{2\mathrm{sinh}(2n+1)\beta + (2n+1)\mathrm{sinh}2\beta}{4\mathrm{sinh}^2(n+1/2)\beta - (2n+1)^2\mathrm{sinh}^2\beta} - 1 \right] \;, \quad (1.1.26)$$

and

$$\eta_\parallel = \eta_0 \left[1 - \frac{9}{16}\xi + \frac{1}{8}\xi^3 - \frac{45}{256}\xi^4 - \frac{1}{16}\xi^5 \right]^{-1} \;, \quad\quad (1.1.27)$$

where $\xi = \frac{a}{z+a}$ and $\beta = \mathrm{cosh}^{-1}(\xi)$. It is possible to simplify the form of $\eta_\perp$ by using a Padé approximation, which is correct up to 1% of accuracy:

$$\eta_\perp = \eta_0 \frac{6z^2 + 9az + 2a^2}{6z^2 + 2az} \;. \quad\quad (1.1.28)$$

Of course, this local viscosity is directly reflected on the diffusive properties of the particle, hence a local diffusion coefficient, which we write:

$$D_i(z) = \frac{k_\mathrm{B}T}{6\pi\eta_i(z)a} \;. \quad\quad (1.1.29)$$

One of the first experimental measurement of the local diffusion coefficient was brought by Faucheux and Libchaber [13] where they measured the mean diffusion coefficient with various gaps and particle radius their results can be found in the Fig.4.
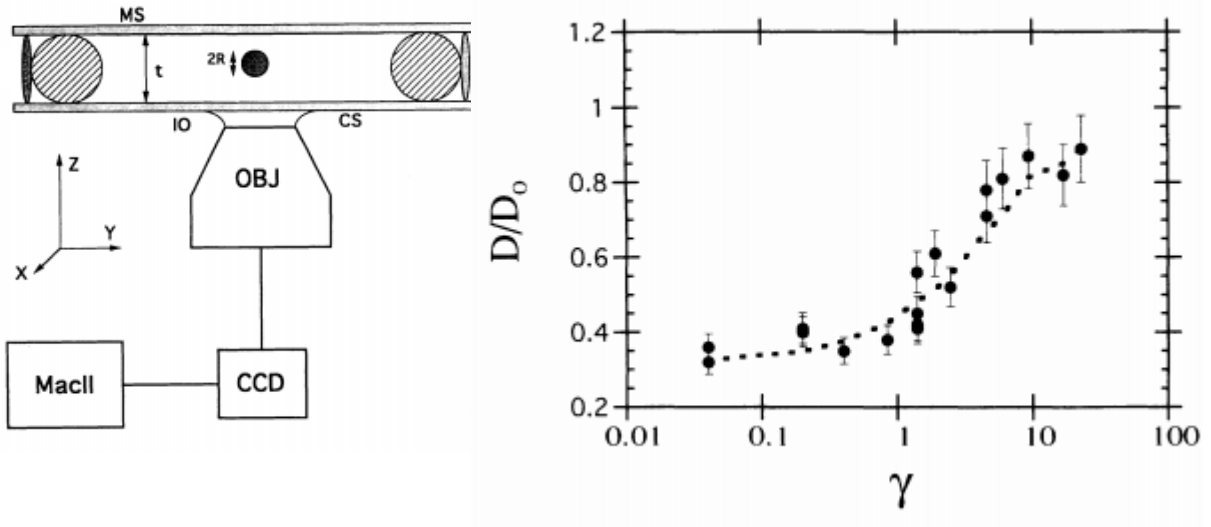
Figure 4: Figure extracted from [13], on the left is the experimental setup used. It is an inverted microscope used in order to track particle of size $2R$ inside a cell of thickness t. On the right is their final result, where they measure the diffusion parallel coefficient $D_\perp$ given by Eq.1.1.27, here normalized by D_0 the bulk diffusion coefficient as a function of γ a confinement constant $\gamma = (\langle z \rangle - a)/a$.
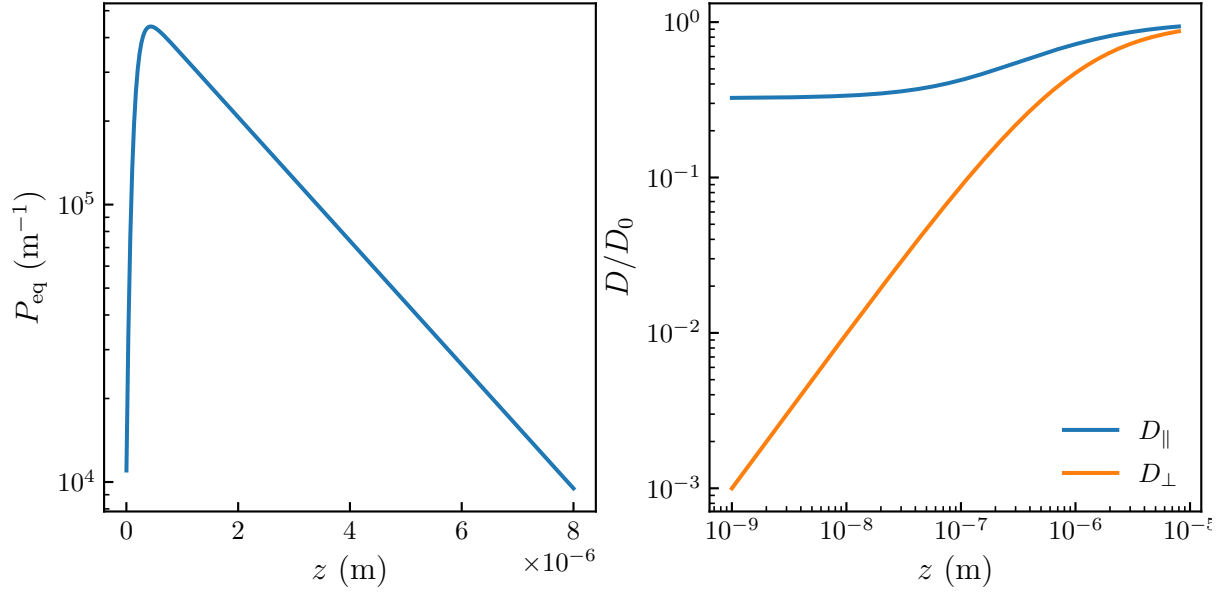
Figure 5: On the left, plot of the Gibbs-Boltzmann distribution Eq.**??** for $a = 1$ μm, $B = 4$, $\ell_{\mathrm{D}} = 100$ nm and $\Delta\rho = 50$ kg.m^{-3}. On the right, local diffusion coefficient normalized by bulk diffusion coefficient $D_0 = k_{\mathrm{B}}T/\gamma$, given by Eq.1.1.27 and Eq.1.1.26
.

1.1.4   Langevin equation for the Brownian motion

1.1.5   Spurious drift

1.1.6   Numerical simulation of confined Brownian motion

1.2   Experimental study

1.2.1   MSD

1.2.2   Non-gaussian dynamics - Displacement distribution

1.2.3   Local diffusion coefficient inference

1.2.4   Precise potential inference using multi-fitting technique

1.2.5   Measuring external forces using the local drifts

1.3   conclusion

References

[1] R. Baraniuk, D. Donoho, and M. Gavish, "The science of deep learning", Proceedings of the National Academy of Sciences **117**, Publisher: National Academy of Sciences Section: Introduction, 30029–30032 (2020).

[2] B. Lemieux, A. Aharoni, and M. Schena, "Overview of DNA chip technology", Molecular Breeding **4**, 277–289 (1998).

[3] Á. Ríos, M. Zougagh, and M. Avila, "Miniaturization through lab-on-a-chip: utopia or reality for routine laboratories? a review", Analytica Chimica Acta **740**, 1–11 (2012).

[4] A. Einstein, "Über die von der molekularkinetischen Theorie der Wärme geforderte Bewegung von in ruhenden Flüssigkeiten suspendierten Teilchen", Annalen der Physik **vol. 4, t. 17** (1905).

[5] J. Perrin, *Les Atomes*, Google-Books-ID: A0ltBQAAQBAJ (CNRS Editions, Nov. 14, 2014), 199 pp.

[6] B. U. Felderhof, "Effect of the wall on the velocity autocorrelation function and long-time tail of brownian motion [†]", The Journal of Physical Chemistry B **109**, 21406–21412 (2005).

[7] M. V. Chubynsky and G. W. Slater, "Diffusing diffusivity: a model for anomalous, yet brownian, diffusion", Physical Review Letters **113**, 098302 (2014).

[8] A. V. Chechkin, F. Seno, R. Metzler, and I. M. Sokolov, "Brownian yet non-gaussian diffusion: from superstatistics to subordination of diffusing diffusivities", Physical Review X **7**, 021002 (2017).

[9] C. I. Bouzigues, P. Tabeling, and L. Bocquet, "Nanofluidics in the debye layer at hydrophilic and hydrophobic surfaces", Physical Review Letters **101**, Publisher: American Physical Society, 114503 (2008).

[10] L. Joly, C. Ybert, and L. Bocquet, "Probing the nanohydrodynamics at liquid-solid interfaces using thermal motion", Physical Review Letters **96**, Publisher: American Physical Society, 046101 (2006).

[11] J. Mo, A. Simha, and M. G. Raizen, "Brownian motion as a new probe of wettability", The Journal of Chemical Physics **146**, Publisher: American Institute of Physics, 134707 (2017).

[12] E. R. Dufresne, T. M. Squires, M. P. Brenner, and D. G. Grier, "Hydrodynamic coupling of two brownian spheres to a planar surface", Physical Review Letters **85**, Publisher: American Physical Society, 3317–3320 (2000).

[13] L. P. Faucheux and A. J. Libchaber, "Confined brownian motion", Physical Review E **49**, 5158–5163 (1994).

[14] E. R. Dufresne, D. Altman, and D. G. Grier, "Brownian dynamics of a sphere between parallel walls", EPL (Europhysics Letters) **53**, Publisher: IOP Publishing, 264 (2001).

[15] H. B. Eral, J. M. Oh, D. v. d. Ende, F. Mugele, and M. H. G. Duits, "Anisotropic and hindered diffusion of colloidal particles in a closed cylinder", Langmuir **26**, Publisher: American Chemical Society, 16722–16729 (2010).

[16] P. Sharma, S. Ghosh, and S. Bhattacharya, "A high-precision study of hindered diffusion near a wall", Applied Physics Letters **97**, Publisher: American Institute of Physics, 104101 (2010).

[17] J. Mo, A. Simha, and M. G. Raizen, "Broadband boundary effects on brownian motion", Physical Review E **92**, 062106 (2015).

[18] M. Matse, M. V. Chubynsky, and J. Bechhoefer, "Test of the diffusing-diffusivity mechanism using near-wall colloidal dynamics", Physical Review E **96**, 042604 (2017).

[19] D. C. Prieve, "Measurement of colloidal forces with TIRM", Advances in Colloid and Interface Science **82**, 93–125 (1999).

[20] A. Banerjee and K. Kihm, "Experimental verification of near-wall hindered diffusion for the brownian motion of nanoparticles using evanescent wave microscopy", Physical review. E, Statistical, nonlinear, and soft matter physics **72**, 042101 (2005).

[21] S. Sainis, V. Germain, and E. Dufresne, "Statistics of particle trajectories at short time intervals reveal fN-scale colloidal forces", Physical review letters **99**, 018303 (2007).

[22] G. Volpe, L. Helden, T. Brettschneider, J. Wehr, and C. Bechinger, "Influence of noise on force measurements", Physical Review Letters **104**, 170602 (2010).

[23] M. Li, O. Sentissi, S. Azzini, G. Schnoering, A. Canaguier-Durand, and C. Genet, "Subfemtonewton force fields measured with ergodic brownian ensembles", Physical Review A **100**, 063816 (2019).

[24] S. K. Sainis, V. Germain, and E. R. Dufresne, "Statistics of particle trajectories at short time intervals reveal fN-scale colloidal forces", Physical Review Letters **99**, 018303 (2007).

[25] B. Robert, "XXVII. a brief account of microscopical observations made in the months of june, july and august 1827, on the particles contained in the pollen of plants; and on the general existence of active molecules in organic and inorganic bodies", The Philosophical Magazine **4**, Taylor & Francis, 161–173 (1828).

[26] S. Peter, "Brownian motion", **Brownian motion**.

[27] J. Perrin, "Mouvement brownien et molécules", J. Phys. Theor. Appl. **9**, 5–39 (1910).

[28] A. Genthon, "The concept of velocity in the history of brownian motion", The European Physical Journal H **45**, 49–105 (2020).

[29] P. Langevin, "Sur la théorie du mouvement brownien", C. R. Acad. Sci. (Paris) 146, 530–533 **65**, 1079–1081 (1908).

[30] R. Durrett, *Probability: theory and examples*, 5th ed., Cambridge Series in Statistical and Probabilistic Mathematics (Cambridge University Press, Cambridge, 2019).

[31] D. Freedman and P. Diaconis, "On the histogram as a density estimator:l 2 theory", Zeitschrift für Wahrscheinlichkeitstheorie und Verwandte Gebiete **57**, 453–476 (1981).

[32] C. Fabry and A. Pérot, "Théorie et application d'une nouvelle méthode de spectroscopie interferentielle.", Ann. Chim. Phys., 7 (1899).

[33] A. Perot and C. Fabry, "On the application of interference phenomena to the solution of various problems of spectroscopy and metrology", The Astrophysical Journal **9**, 87 (1899).

[34] A. A. Michelson and E. W. Morley, "On the relative motion of the earth and the luminiferous ether", American Journal of Science **s3-34**, Publisher: American Journal of Science Section: Extraterrestrial geology, 333–345 (1887).

[35] LIGO Scientific Collaboration and Virgo Collaboration et al., "GW151226: observation of gravitational waves from a 22-solar-mass binary black hole coalescence", Physical Review Letters **116**, in collab. with B. P. Abbott, Publisher: American Physical Society, 241103 (2016).

[36] A. S. Curtis, "THE MECHANISM OF ADHESION OF CELLS TO GLASS. a STUDY BY INTERFERENCE REFLECTION MICROSCOPY", The Journal of Cell Biology **20**, 199–215 (1964).

[37] T. J. Filler and E. T. Peuker, "Reflection contrast microscopy (RCM): a forgotten technique?", The Journal of Pathology **190**, 635–638 (2000).

[38] P. A. Siver and J. Hinsch, "THE USE OF INTERFERENCE REFLECTION CONTRAST IN THE EXAMINATION OF DIATOM VALVES", Journal of Phycology **36**, 616–620 (2000).

[39] I. Weber, "[2] reflection interference contrast microscopy", in *Methods in enzymology*, Vol. 361, Biophotonics, Part B (Academic Press, Jan. 1, 2003), pp. 34–47.

[40] L. Limozin and K. Sengupta, "Quantitative reflection interference contrast microscopy (RICM) in soft matter and cell adhesion", Chemphyschem: A European Journal of Chemical Physics and Physical Chemistry **10**, 2752–2768 (2009).

[41] F. Nadal, A. Dazzi, F. Argoul, and B. Pouligny, "Probing the confined dynamics of a spherical colloid close to a surface by combined optical trapping and reflection interference contrast microscopy", Applied Physics Letters **79**, 3887–3889 (2002).

[42] J. Raedler and E. Sackmann, "On the measurement of weak repulsive and frictional colloidal forces by reflection interference contrast microscopy", Langmuir **8**, 848–853 (1992).

[43] H. S. Davies, D. Débarre, N. El Amri, C. Verdier, R. P. Richter, and L. Bureau, "Elastohydrodynamic lift at a soft wall", Physical Review Letters **120**, 198001 (2018).

[44] C. F. Bohren and D. R. Huffman, *Absorption and scattering of light by small particles* (Wiley, Apr. 1998).

[45] H. J. W. Strutt, "LVIII. on the scattering of light by small particles", The London, Edinburgh, and Dublin Philosophical Magazine and Journal of Science **41**, Publisher: Taylor & Francis _eprint: https://doi.org/10.1080/14786447108640507, 447–454 (1871).

[46] L. Lorenz, *Lysbevægelsen i og uden for en af plane Lysbølger belyst Kugle*, Google-Books-ID: hnE7QwAACAAJ (1890), 62 pp.

[47] G. Mie, "Beiträge zur optik trüber medien, speziell kolloidaler metallösungen", Annalen der Physik **330**, _eprint: https://onlinelibrary.wiley.com/doi/pdf/10.1002/andp.19083300302 377–445 (1908).

[48] B. Ovryn and S. H. Izen, "Imaging of transparent spheres through a planar interface using a high-numerical-aperture optical microscope", Journal of the Optical Society of America A **17**, 1202 (2000).

[49] S.-H. Lee, Y. Roichman, G.-R. Yi, S.-H. Kim, S.-M. Yang, A. v. Blaaderen, P. v. Oostrum, and D. G. Grier, "Characterizing and tracking single colloidal particles with video holographic microscopy", Optics Express **15**, Publisher: Optical Society of America, 18275–18282 (2007).

[50] J. Katz and J. Sheng, "Applications of holography in fluid mechanics and particle dynamics", Annual Review of Fluid Mechanics **42**, _eprint: https://doi.org/10.1146/annurev-fluid-121108-145508, 531–555 (2010).

[51] P. Gregory, *Bayesian logical data analysis for the physical sciences: a comparative approach with mathematica® support*, Google-Books-ID: idkLAQAAQBAJ (Cambridge University Press, Apr. 14, 2005), 496 pp.

[52] T. G. Dimiduk and V. N. Manoharan, "Bayesian approach to analyzing holograms of colloidal particles", Optics Express **24**, Publisher: Optical Society of America, 24045–24060 (2016).

[53] W. J. Lentz, "Generating bessel functions in mie scattering calculations using continued fractions", Applied Optics **15**, Publisher: Optical Society of America, 668–671 (1976).

[54] J. Fung and V. N. Manoharan, "Holographic measurements of anisotropic three-dimensional diffusion of colloidal clusters", Physical Review E **88**, 020302 (2013).

[55] A. Wang, T. G. Dimiduk, J. Fung, S. Razavi, I. Kretzschmar, K. Chaudhary, and V. N. Manoharan, "Using the discrete dipole approximation and holographic microscopy to measure rotational dynamics of non-spherical colloidal particles", Journal of Quantitative Spectroscopy and Radiative Transfer **146**, 499–509 (2014).

[56] R. W. Perry, G. Meng, T. G. Dimiduk, J. Fung, and V. N. Manoharan, "Real-space studies of the structure and dynamics of self-assembled colloidal clusters", Faraday Discussions **159**, Publisher: The Royal Society of Chemistry, 211–234 (2013).

[57] T. G. Dimiduk, R. W. Perry, J. Fung, and V. N. Manoharan, "Random-subset fitting of digital holograms for fast three-dimensional particle tracking", Applied Optics **53**, G177 (2014).

[58] A. Yevick, M. Hannel, and D. G. Grier, "Machine-learning approach to holographic particle characterization", Optics Express **22**, 26884 (2014).

[59] M. D. Hannel, A. Abdulali, M. O'Brien, and D. G. Grier, "Machine-learning techniques for fast and accurate feature localization in holograms of colloidal particles", Optics Express **26**, Publisher: Optical Society of America, 15221–15231 (2018).

[60] L. E. Altman and D. G. Grier, "CATCH: characterizing and tracking colloids holographically using deep neural networks", The Journal of Physical Chemistry B **124**, Publisher: American Chemical Society, 1602–1610 (2020).

[61] L. Wilson and R. Zhang, "3d localization of weak scatterers in digital holographic microscopy using rayleigh-sommerfeld back-propagation", Optics Express **20**, 16735 (2012).

[62] J. W. Goodman, *Introduction to fourier optics*, Google-Books-ID: ow5xs_Rtt9AC (Roberts and Company Publishers, 2005), 520 pp.

[63] F. C. Cheong, B. J. Krishnatreya, and D. G. Grier, "Strategies for three-dimensional particle tracking with holographic video microscopy", Optics Express **18**, Publisher: Optical Society of America, 13563–13573 (2010).

[64] G. C. Sherman, "Application of the convolution theorem to rayleigh's integral formulas", JOSA **57**, Publisher: Optical Society of America, 546–547 (1967).

[65] U. Schnars and W. P. Jüptner, "Digital recording and reconstruction of holograms in hologram interferometry and shearography", Applied Optics **33**, 4373–4377 (1994).

[66] T. M. Kreis, "Frequency analysis of digital holography with reconstruction by convolution", Optical Engineering **41**, Publisher: International Society for Optics and Photonics, 1829–1839 (2002).

[67] J. J. Moré, "The levenberg-marquardt algorithm: implementation and theory", in Numerical analysis, edited by G. A. Watson, Lecture Notes in Mathematics (1978), pp. 105–116.

[68] J. N. Israelachvili, *Intermolecular and surface forces*, Google-Books-ID: MVbWB-hubrgIC (Academic Press, May 29, 2015), 706 pp.

[69] G. M. Bell, S. Levine, and L. N. McCartney, "Approximate methods of determining the double-layer free energy of interaction between two charged colloidal spheres", Journal of Colloid and Interface Science **33**, 335–359 (1970).

[70] S. H. Behrens and D. G. Grier, "The charge of glass and silica surfaces", The Journal of Chemical Physics **115**, 6716–6721 (2001).

[71] H. Faxen, "Fredholm integral equations of hydrodynamics of liquids i", Ark. Mat., Astron. Fys **18**, 29–32 (1924).